Research Article

Hongrui Wang, Wei Ling, Jizhong Chen, Zhian Wang, Xian-Xiang Zeng, Yongqing Hu, Xiongwei Wu, Qi Deng*, Guanghui Chen*, Yuping Wu*, and Rudolf Holze

A three-dimensional conducting network of rGO-in-graphite-felt as electrode for vanadium redox flow batteries

https://doi.org/10.1515/eetech-2018-0008
Received Feb 09, 2018; accepted Oct 19, 2018

Abstract: Graphite felt (GF) with numerous merits has been widely used as electrode in all-vanadium redox flow batteries (VRFB), but its further application is still hindered by its intrinsically poor electrocatalytic activity. Herein, we propose a three-dimensional (3D) conducting network constructed with reduced graphene oxide (rGO) in the GF electrode via a two-step method. The 3D conducting network with abundant oxygen-containing functional groups in the GF is conducive to the transport of electrons between GF fibers and the electrochemical charge transfer to vanadium ions in the composite electrode; it can enhance the electrocatalytic activity and conductivity of GF. The VRFB using 3D rGO modified GF (mGF) electrode exhibited outstanding energy efficiency of 73.4% at a current density of 100 $mA{\cdot}cm^{-2}$, which is much higher than that with pristine GF (pGF) (65.4%); and better rate capability. These first results reveal that GF with 3D conducting network shows promising opportunities for the VRFB and other electrochemical flow systems.

Keywords: Vanadium redox flow battery; electrode; reduced graphene oxide; three-dimensional conducting; network

1 Introduction

With the over-utilization of fossil fuels and its impact on environmental pollution, clean and renewable energy sources have attracted great attention [1]. However, many renewable energy sources, such as solar, wind, tidal energy, show wildly fluctuating availability, which impedes further application of these energy sources [2]. To overcome this major shortcoming large-scale energy storage systems are an ideal match because they can meet even fast changes in energy supply and can also ameliorate discrepancies of supply and demand [3]. Among available energy storage technologies, including Li ion battery [4, 5], Na ion battery [6], Na-S battery [7] supercapacitors [8], and redox flow batteries [9, 10] the all-vanadium redox flow battery (VRFB) is regarded as the most promising large-scale energy storage systems due to its long cycle life, good safety, and low maintenance cost [11–13]. The electrode is the central component of the VRFB providing the reaction zone for vanadium redox reactions. The energy efficiency of the VRFB is limited mostly by the electrochemical charge transfer and diffusion polarization of the electrodes. Among many different electrode

***Corresponding Author: Qi Deng:** College of Science, College of Agronomy, Hunan Agricultural University, Changsha 410128, China; Email: dengqibq@163.com
***Corresponding Author: Guanghui Chen:** College of Science, College of Agronomy, Hunan Agricultural University, Changsha 410128, China; State Key Laboratory of Operation and Control of Renewable Energy & Storage Systems, China Electric Power Research Institute, Beijing 100192, China; Email: cgh68@163.com
***Corresponding Author: Yuping Wu:** College of Science, College of Agronomy, Hunan Agricultural University, Changsha 410128, China; State Key Laboratory of Materials-Oriented Chemical Engineering, and School of Energy Science and Engineering, Nanjing Tech University, Nanjing 211816, Jiangsu Province, China; Email: wuyp@fudan.edu.cn
Hongrui Wang, Wei Ling: College of Science, College of Agronomy, Hunan Agricultural University, Changsha 410128, China. These authors contributed equally
Jizhong Chen: State Key Laboratory of Operation and Control of Renewable Energy & Storage Systems, China Electric Power Research Institute, Beijing 100192, China
Zhian Wang: School of Chemistry and Chemical Engineering, Central South University, Changsha 410083, China
Xian-Xiang Zeng: College of Science, College of Agronomy, Hunan Agricultural University, Changsha 410128, China
Yongqing Hu: Hunan Province YinFeng New Energy Co. LTD, Changsha, 410000, P. R. China
Xiongwei Wu: College of Science, College of Agronomy, Hunan Agricultural University, Changsha 410128, China; Hunan Province YinFeng New Energy Co. LTD, Changsha, 410000, P. R. China
Rudolf Holze: Technische Universität Chemnitz, Institut für Chemie, AG Elektrochemie, 09107 Chemnitz, Germany

materials carbon-based materials especially graphite felt (GF) is widely applied in the electrodes for VRFB due to its low cost, excellent acid resistance and mechanical strength [14]. However, its low conductivity and poor electrocatalytic activity are insufficient for VRFBs. Therefore, many methods such as surface functionalization, metal and metal oxide deposition, and heteroatom doping have been adopted to improve the GF performance. Surface functionalization methods including heat and acid treatments [15, 16] and electrochemical oxidation [17] are effective to improve the electrochemical activity via introducing oxygen-containing functional groups into the GF. However, supported by the flowing electrolyte solution the oxygen-containing functional groups are easily lost from the GF; this causes major deterioration of stable battery performance. Precious metals deposited on the GF, such as Pt, Pd, Ir, Au, Ru, have been proven as effective electrocatalysts for vanadium redox reactions [18], but their cost should be taken into consideration, and some of them are prone to cause gas evolution by electrolyte solution decomposition, giving rise to a low coulombic efficiency. Other low-cost metals and metal oxides, such as Bi, Mn_3O_4, WO_3, ZrO_2, MoO_3, have been reported to boost the electrochemical performance of VRFB [19–24], but their acid resistance needs further improvement. Nitrogen doping of the GF can alter the charge distribution surrounding adjacent carbon atoms [25] and accelerate the rate of vanadium redox reactions on the GF electrode. Carbon nanotubes [26] and carbon nanofiber-modified GF [27] show excellent electrocatalytic activity towards the VO_2^+/VO^{2+} couple due to their high electrical conductivity and large electrochemically active surface area, but the preparation process is too tedious for general application. Graphene is widely applied in the field of electrochemical energy storage [28] due to its remarkable conductivity and large surface area that provides extended surface for vanadium redox reactions and conceivably for further functionalization [29]. Graphene oxide (GO), as a derivative of graphene, contains significant amounts of hydroxyl and carboxylic acid groups [30], but suffers from conductivity reduction after introduction of functional groups [31, 32]. Consequently, it is still desirable to construct interconnected structures with optimized conductivity and numerous electrocatalytically active sites.

In this paper, we propose a two-step method including hydrothermal and annealing processes to fabricate three-dimensional (3D) conducting networks of reduced graphene oxide (rGO) in GF, which not only retains a large fraction of the oxygen-containing functional groups as active sites, but also restores defects caused by the oxidation of graphene to an optimized extent. The 3D conducting network in the GF facilitates the transport of electrons between GF fibers and supports the charge transfer of vanadium ions inside the composite electrode, thus enhancing electrocatalytic activity and conductivity of GF.

2 Methods

2.1 Preparation of mGF with 3D conducting network

First, GO was prepared by the oxidation of graphite flakes (> 99.99%, Alfa Aesar) using an improved Hummers method [33]. The prepared GO was diluted to 3.2 $g{\cdot}L^{-1}$ with deionized water. The pristine graphite felt (pGF) (25 mm × 25 mm × 6 mm, Yingfeng new energy Co. Ltd, China) was immersed into 30 mL GO solution and ultrasonicated for 15 minutes to obtain a homogeneous dispersion. The mixture was transferred into a 100 mL Teflon-lined autoclave and heated to 180°C for 5 h. After cooling to room temperature, the samples were freeze-dried for 24 h. Subsequently, the samples were placed in a quartz tube for annealing at 400°C (rate 5°C min^{-1}) under argon atmosphere for 1h. After cooling to room temperature, the modified graphite felt (mGF) was obtained.

2.2 Characterization

The samples were assessed with a scanning electron microscope (SEM, JEOL 6701F) and Fourier Transform infrared (FTIR) microspectroscopy (Thermo Fisher, iN10-iZ10). Cyclic voltammetry (CV) tests were conducted in a three-electrode system (Chenghua CHI760D). A platinum and a silver chloride electrode (Ag/AgCl) were used as the counter and reference electrodes, respectively. The mGF and pGF served as the working electrodes (0.5 cm × 0.5 cm). The electrolyte was 0.05 $mol{\cdot}L^{-1}$ $VOSO_4$ in 3 $mol{\cdot}L^{-1}$ H_2SO_4. Electrode impedance (EIS) was measured by an Autolab (PGSTAT 302N) electrochemical workstation with 5 mV amplitude sine wave in the frequency range 0.01 Hz - 100 kHz at open circuit potential. The obtained data were fitted using ZView software. Thegalvanostatic tests were conducted on a battery test system (Land CT2001A). The positive and negative electrode area were 4 cm^2, the electrolyte solution contained 0.75 $mol{\cdot}L^{-1}$ $VOSO_4$ + 0.375 $mol{\cdot}L^{-1}V_2(SO_4)_3$ in aqueous 3 $mol{\cdot}L^{-1}$ H_2SO_4 (15 mL) on both sides (Yinfeng new energy Co. Ltd), a Nafion 115 membrane (DuPont) was used as a separator. The cells were charged to 1.6 V and discharged to 0.8 V.

For conductivity tests, the sample (20 mm × 20 mm × 6 mm) was sandwiched between two copper foils, the compression ratio and resistance data were collected with a micrometer caliper and a multimeter.

3 Results and Discussion

The pristine graphite felt (pGF) fibers have a smooth surface (Figure 1a and 1b). In contrast, a 3D network is visible within the modified graphite felt (mGF) (Figure 1c and 1d) indicating the successful interconnection by the rGO. An SEM-image of the rGO is displayed in Figure 1e. A schematic illustration of the 3D conducting network is shown in Figure 1f. The 3D conducting network structure increases the number of channels for electron transfer and the interfacial contact area between mGF and vanadium electrolyte solution significantly improving the electrochemical performance of the mGF.

The functional groups of the pGF and mGF were characterized by Fourier Transform infrared (FTIR) spectroscopy (Figure 2). With pGF, only a weak absorbance peak appears at 2365 cm^{-1} corresponding to a C-OH stretching mode. mGF shows four strong peaks at 2370 cm^{-1}, 1747 cm^{-1}, 1593 cm^{-1} and 1246 cm^{-1} attributed to C-OH, C=O, COOH and C-O modes, respectively.In addition, the C-OH, C=O and C-O-C functional groups were observed from the FT-IR curve of rGO located at 3414 cm^{-1}, 1600 cm^{-1} and 1014 cm^{-1}, respectively. Obviously, mGF contains more active sites signaled by vibrational modes when compared with pGF, implying improved electrocatalytic activity of the mGF electrode. To verify the conductivity of the network constructed by 3D rGO, test results of electronic conductivityof the GF under different compression ratios are shown in Figure 2b. The ohmic resistance of the pGF is nearly 6 times higher than that of the mGF at a low compression ratio (2%), which indicates substantially improved electronic conductivity of mGF. With increasing compression ratio, the ohmic resistance of mGF changes only slightly, revealing that mGF can maintain a constant and high electronic conductivity compared with pGF.

Cyclic voltammetry (CV) was used to evaluate the electrochemical performance of the pGF and mGF with the positive and negative redox couples. At the scan rate of 10 mV s^{-1}, the ratio of oxidation peak current (I_{pa}) and

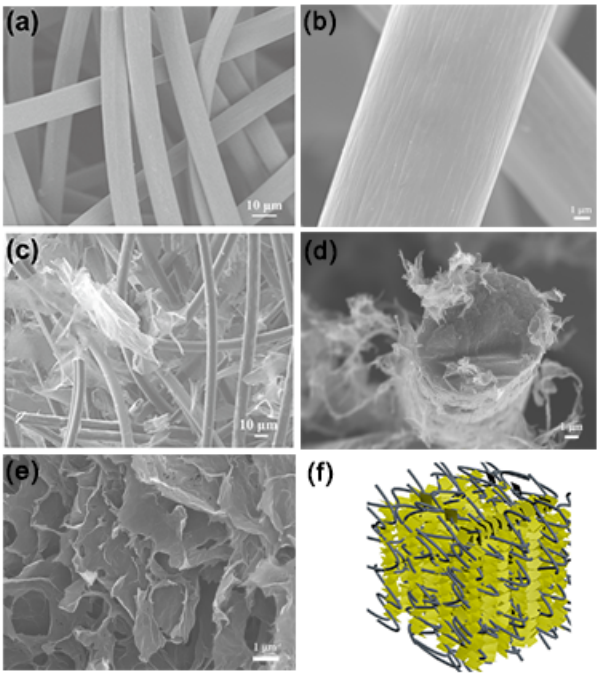

Figure 1: SEM images of the pGF with low (a) and high (b) magnifycations and mGF with low (c) and high (d) magnifications and rGO (e). (f) Schematic illustration of the 3D conducting network.

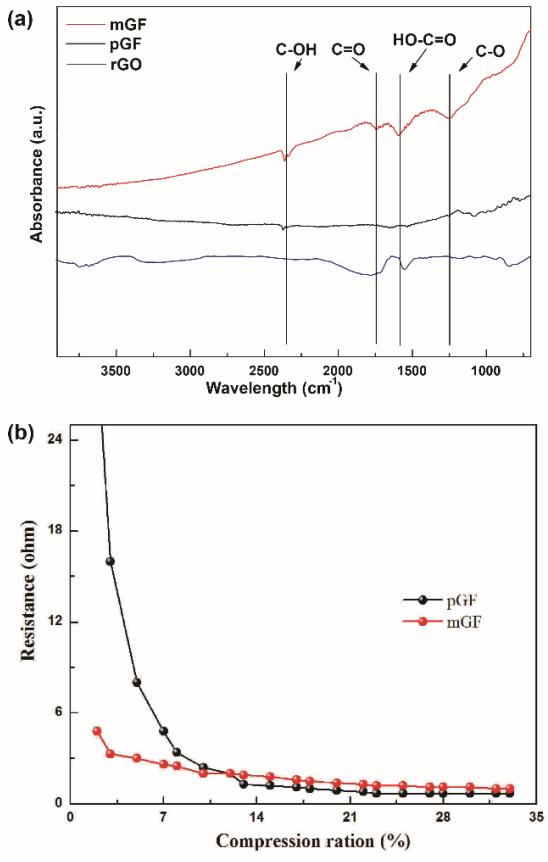

Figure 2: (a) FTIR spectra of the pGF, mGF and rGO, (b) conductivities of pGF and mGF at different compression ratio curves.

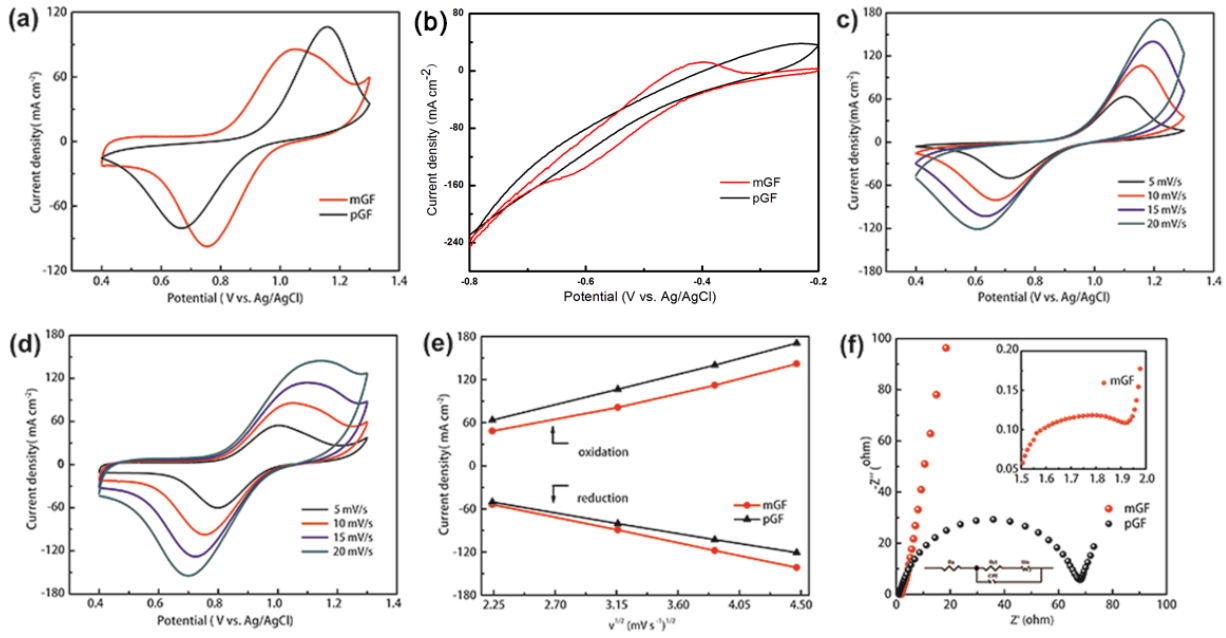

Figure 3: CV curves of the pGF and mGF towards (a) VO_2^+/VO^{2+} and (b) V^{3+}/V^{2+} redox couples in 0.05 M $VOSO_4$ in 3 M H_2SO_4 at the scan rate of 10 mV s^{-1}. CV curves of (c) pGF and (d) mGF under different scan rates ranging from 5 to 20 mV·s^{-1} for VO_2^+/VO^{2+} redox reactions. (e) Plot of oxidation peak current (I_{pa}) and reduction peak current (I_{pc}) versus square root of scan rate for VO_2^+/VO^{2+} redox reactions. (f) EIS plots for pGF and mGF, inset: enlarged high frequency part with mGF and the corresponding equivalent circuit diagram.

reduction peak current (I_{pc}) density for the mGF electrode (I_{pa}/I_{pc} = 0.88) is much closer to 1 than that for pGF (I_{pa}/I_{pc} = 1.32) for the positive redox reaction (Figure 3a), which indicates that mGF improves reversibility for theVO_2^+/VO^{2+} redox couple. In addition, the positive peak potential separation of the mGF (ΔE = 287 mV) decreases by 188 mV compared with pGF indicating substantially improved electrocatalytic activity of the mGF towards the positive redox reaction. With pGF and mGF dramatic differences also for the negative redox couple can be observed. No obvious oxidation and reduction peaks appear for the pGF because of the occurrence of hydrogen evolution (Figure 3b), which greatly affects the battery efficiency. On the contrary, the mGF presents distinct oxidation and reduction peaks for the negative redox couple, implying that mGF has also considerably enhanced electrochemical activity for the V^{2+}/V^{3+} couple.

CVs of pGF (Figure 3c) and mGF (Figure 3d) at different scan rates for the positive redox couple were recorded. With increasing scan rate the onset potential and peak potential separation with mGF presents only minor variations compared with that for pGF, demonstrating lower polarization for theVO_2^+/VO^{2+} redox reaction at mGF. Following from the linear relationship between the peak current and square root of scan rate plotted according to the Randles-Sevcik equation the redox reaction VO_2^+/VO^{2+} is diffusion-controlled (Figure 3e) [34]. Whereas the slopes of plots for the oxidation peaks are hardly different, the slope for the reduction process on the mGF is slightly larger than for pGF, indicating a faster mass transport of the oxidized species or a slightly changed active surface area caused by *e.g.* changed wetting. These overall improvements are attributed to the 3D conducting network in mGF that greatly enhances the contact area between the electrode and electrolyte solution and reduces the charge transfer resistance (R_{ct}), which was verified by the electrochemical impedance (EIS) measurements. As shown in the Nyquist plot (Figure 3f), there is a semicircle in the high frequency range due to R_{ct} an C_{DL} for the VO_2^+/VO^{2+} reaction, and a sloped line in the low frequency region arising from diffusion through electrolyte solution, indicating that vanadium redox reactions are subject to mixed controlled by mass diffusion and charge transfer [35]. After fitting through ZView software, the R_{ct} value for pGF and mGF were approximately 67.3 Ω and 0.460 Ω, respectively. The prominent reduction of R_{ct} for mGF is ascribed to the abundant oxygen-containing groups, serving as active sites for vanadium redox reaction. Thus, the 3D conducting network in the mGF effectively improves the conductivity and electrocatalytic activity of the electrode through enhanced electron transfer and number of active sites for the vanadium redox reaction on the surface of mGF.

A VRFB single cell was assembled with mGF electrodes. Charge-discharge tests were performed with cell

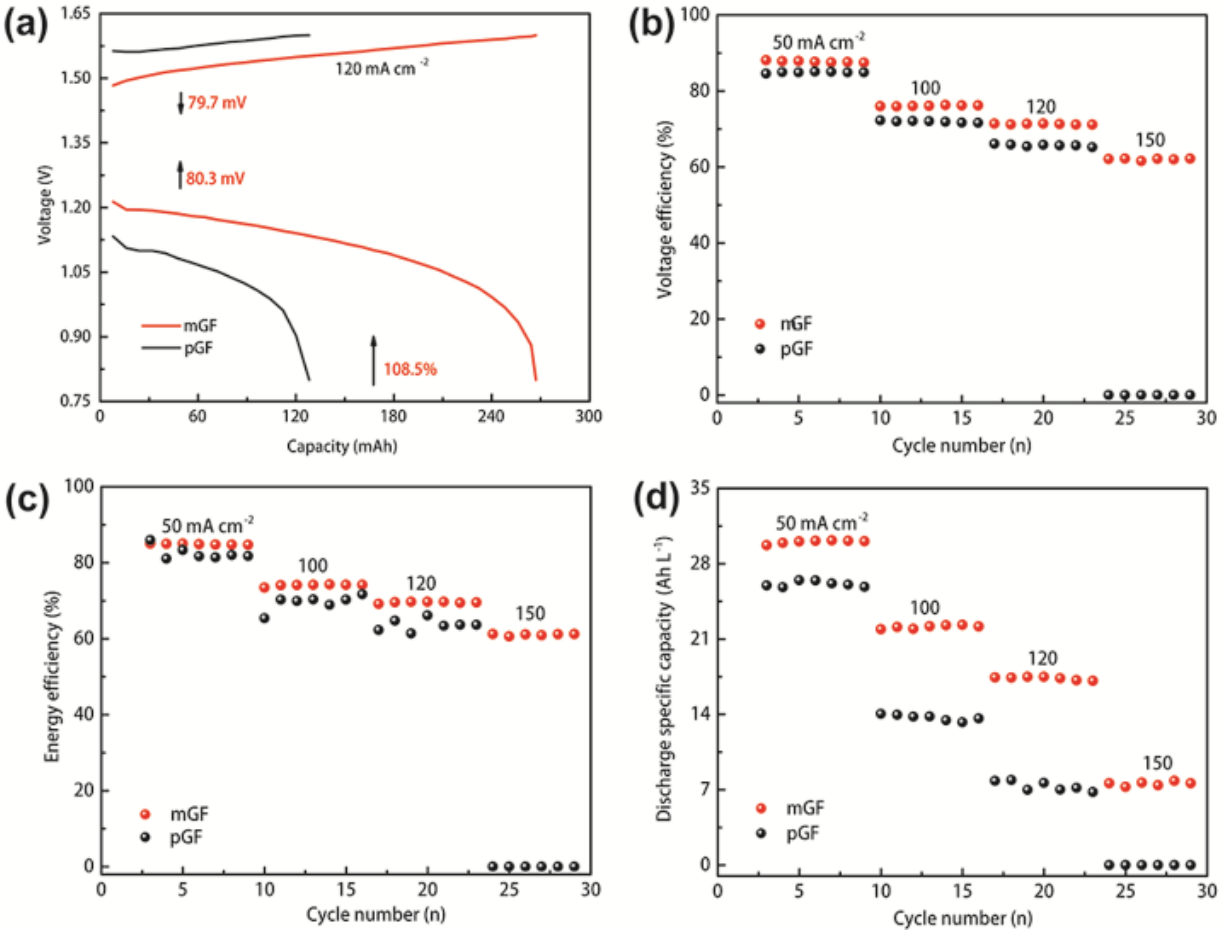

Figure 4: (a) The voltage profiles of pGF and mGF electrodes at the current density of 120 mA cm^{-2}, (b) voltage efficiency, (c) energy efficiency and (d) discharge capacity at different current densities from 50 to 150 mA cm^{-2}.

voltage ranging from 0.8 V to 1.6 V. Compared with the pGF-containing cell (Figure 4a), the mGF-containing cell exhibits a lower charging plateau and a higher discharging plateau, and the corresponding overvoltage decreased by 160 mV. In addition, the specific discharge capacity of the mGF-containing cell is 109% higher than that with pGF at the current density of 120 mA·cm^{-2}. This result confirms that the vanadium redox reactions at mGF has a smaller electrochemical polarization during the charge-discharge process compared with pGF, which is associated with more active sites and larger electrode/electrolyte interfacial contact area, promoting the charge transfer for the redox reactions. The voltage efficiency (VE) and energy efficiency (EE) are two important parameters for the VRFB. The VE value with mGF is 71.4% at the current density of 120 mA·cm^{-2} (Figure 4b), whereas it is only 66.1% with pGF, indicating a lower polarization effect for the mGF. The EE value of VRFB using pGF is 61.4% at 120 mA·cm^{-2}, the battery fails at 150 mA·cm^{-2} (Figure 4c). However, the EE values of mGF-based VRFB were 85.0% and 61.9% at current densities of 50 and 150 mA·cm^{-2}, respectively. The EE values of the mGF are more stable than those with pGF at the same current density, which also implies the mGF exhibits a good cycling stability. The specific discharge capacity of VRFB using mGF was 17.1 Ah·L^{-1} at j = 120 mA·cm^{-2}, which is 2.5 times higher than that with pGF (6.79 Ah·L^{-1}). At 150 mA·cm^{-2} the pGF-based VRFB can't work, but the VRFB with mGF still releases a specific discharge capacity of 7.83 Ah·L^{-1} (Figure 4d). The much higher rate performance of VRFB is attributed to the greatly improved electrocatalytic activity.

In summary, we propose a two-step method including hydrothermal and annealing processes to fabricate a 3D conducting network constructed of rGO in the GF, which not only provides abundant oxygen-containing groups serving as active sites for vanadium redox reactions, but also enhances the electron transport providing improved electro-catalytic activity and conductivity. The EE of VRFB with mGF was 12.3% higher than that with pGF electrode at 100 mA·cm^{-2}, this electrode works sturdily even at 150

$mA \cdot cm^{-2}$. The elaborately designed 3D conducting network reveals its effectiveness in tackling the chronic issues with VRFB, and highlights its great potential for other electrochemical flow systems.

Acknowledgement: This work was supported by the Distinguished Young Scientists Program of the National Natural Science Foundation of China (No. 51425301 and U1601214), the National Natural Science Foundation of China (Grant Nos. 51772093), and the Beijing National Laboratory for Molecular Sciences (Grant No. BNLMS20150118).

References

[1] Chu S., Cui Y., Liu N., Nat. Mater., 2016, 16, 16-22
[2] Park S., Kim H., J. Mater. Chem. A., 2015, 3, 12276-12283
[3] Ulaganathan M., Aravindan V., Yan Q., Madhavi S., Skyllas-Kazacos M., Lim T.M., Adv. Mater. Inter., 2016, 3, 1500309
[4] Wang F., Wu X.W., Li C., Zhu Y., Fu L., Wu Y., Liu X., Energy Environ. Sci., 2016, 9, 3570-3611
[5] Wu X.W., Xie H., Deng Q., Wang H.X., Sheng H., Yin Y.X., Zhou W.X., Li R.L., Guo Y.G., ACS App. Mater. Interfaces., 2017, 9, 1553-1561
[6] Longoni G., Pena Cabrera R.L., Polizzi S., D'Arienzo M., Mari C.M., Cui Y., Ruffo R., Nano Lett., 2017, 17, 992-1000
[7] Yao Y., Zeng L., Hu S., Jiang Y., Yuan B., Yu Y., Small., 2017, 13, 1603513
[8] Zhu L., Wu W., Wang X., Wu X., Tang W., Wu Y.,RSC Adv., 2014, 4, 59088-59093
[9] Hu B., DeBruler C., Rhodes Z., Liu T.L., J. Am. Chem. Soc., 2017, 139, 1207-1214
[10] Schweiss R., Meiser C., Goh F.W.T.,ChemElectroChem., 2017, 4, 1969-1974
[11] Skyllas-Kazacos M., Grossmith F., J. Electrochem. Soc., 1987, 134, 2950-2953
[12] Wu L., Shen Y., Yu L., Xi J., Qiu X., Nano Energy., 2016, 28, 19-28
[13] Deng Q., Huang P., Zhou X.W.X., Ma Q., Zhou N., Xie H., Ling W., Zhou C.J., Yin Y.X., Wu X.W., LuX.Y.,Guo Y.G., Adv. Energy Mater., 2017, 170046
[14] Wu X.W., Yuan X., Wang Z., Liu J., Hu Y., Deng Q., Yin X., Zhou Q., Zhou W., Wu Y., J. Solid State Chem., 2016, 21, 429-435
[15] Sun B., Skyllas-Kazacos M., Electrochim. Acta., 1992, 37, 1253-1260
[16] Sun B., Skyllas-Kazacos M., Electrochim. Acta., 1992, 37, 2459-2465
[17] Men Y., Sun T., Int. J. Electrochem. Sci., 2012, 7, 3482-3488
[18] Kim K.J., Park M.S., Kim Y.J., Kim J.H., Dou S.X., Skyllas-Kazacos M.,J. Mater. Chem. A., 2015, 3, 16913-16933
[19] Li B., Gu M., Nie Z., Shao Y., Luo Q., Wei X., Li X., Xiao J., Wang C., Sprenkle V., Wang W., Nano Lett., 2013, 13, 1330-1335
[20] Ejigu A., Edwards M., Walsh D.A., ACS Catal., 2015, 5, 7122-7130
[21] Kabtamu D.M., Chen J.Y., Chang Y.C., Wang C.H., J. Mater. Chem. A., 2016, 4, 11472-11480
[22] Zhou H., Shen Y., Xi J., Qiu X., Chen L., ACS Appl. Mater. Interfaces., 2016, 8, 15369-15378
[23] Cao L., Skyllas-Kazacos M., Wang D.W., ChemElectroChem., 2017, 4, 1836-1839
[24] Kim K.J., Park M.S., Kim J.H., Hwang U., Lee N.J., Jeong G., Kim Y.J., Chem. Commun., 2012, 48, 5455-5457
[25] Hu L., Sun Y., Zhou Y., Bai L., Zhang Y., Han M., Huang H., Liu Y., Kang Z., Inorg. Chem. Front., 2017, 4, 946-953
[26] Hussain M., Saridara C., Mitra S., RSC Adv., 2011, 1, 685-689
[27] Park M., Jung Y.J., Kim J., Lee H.I., Cho J., Nano Lett., 2013, 13, 4833-4839
[28] Raccichini R., Varzi A., Passerini S., Scrosati B., Nat. Mater., 2015, 14, 271-279
[29] Li W., Zhang Z., Tang Y., Bian H., Ng T.W., Zhang W., Lee C.S., Adv. Sci., 2015, 3, 1500276
[30] Han P., Yue Y., Liu Z., Xu W., Zhang L., Xu H., Dong S., Cui G., Energy Environ. Sci., 2011, 4, 4710-4717
[31] Park M., Jeon I.Y., Ryu J., Baek J.B., Cho J., Adv. Energy Mater., 2015, 5, 1401550
[32] Chakrabarti B., Nir D., Yufit V., Tariq F., Rubio-Garcia J., Maher R., Kucernak A., Aravind P., N. Brandon, ChemElectroChem., 2017, 4, 194-200
[33] Marcano D.C., Kosynkin D.V., Berlin J.M., Sinitskii A., Sun Z., Slesarev A., Alemany L.B., Lu W., Tour J.M., ACS Nano., 2010, 4, 4806-4814
[34] Kabtamu D.M., Chen J.Y., Chang Y.C., Wang C.H., J. Power Sources., 2017, 341, 270-279
[35] Lee H.J., Kil D., Kim H., J. Electrochem. Soc., 2016, 163, A2586-A2591